



Sequestration of Heavy Metals from Water by *Aegle marmelos* (Bael) Leaves as Promising Biomaterial: Kinetic and Equilibrium Studies

INDU RANI^{*b}, SACHIN KUMARI^b, SUSHILA SINGH^b, BHAGYA SHREE^b, MUSKAN^b and MANJU^b

Department of Chemistry, College of Basic Sciences & Humanities, Chaudhary Charan Singh Haryana Agricultural University, Hisar-125004, India

*Corresponding author: E-mail: indu1342@gmail.com

Received: 27 May 2024;

Accepted: 22 July 2024;

Published online: 25 July 2024;

AJC-21718

Heavy metals abatement from polluted water through the use of green biosorbents is a growing research area due to its renewability and inexpensive. This study investigates the idea of utilizing *Aegle marmelos* (Bael) leaves as a biosorbent for the removal of heavy metal ions Cd(II), Pb(II) and Cr(VI) from simulated wastewater. The surface area, functionality, surface morphology and elemental analysis of biosorbent were analyzed by BET, FTIR, FE-SEM with EDX, respectively. Batch studies were done for biosorption of heavy metal ions. The maximum biosorption capacity of heavy metal ions were optimized by varying the pH (2-9), metal ions concentration (20-80 mg/L), biosorbent dose (0.02-0.2 g/L) and contact time (30-210 min). The Langmuir adsorption isotherms and pseudo-second order kinetics models were the most suitable for the biosorption of heavy metal ions and the maximum adsorption capacity was 11.85, 10.35 and 8.55 mg/g for Pb(II), Cd(II) and Cr(VI) heavy metals, respectively at optimized time 120 min. Thermodynamics studies revealed that biosorption of Pb(II), Cd(II) and Cr(VI) on *A. marmelos* biosorbent was exothermic and spontaneous in nature. Finally, the removal efficiency of *A. marmelos* biosorbent against the all three metals were found maximum for Pb(II) followed by Cd(II) and Cr(VI) due to the variations in hydration energy of these heavy metals.

Keywords: Biosorption, *Aegle marmelos*, Heavy metals, Batch studies, Adsorption capacity.

INTRODUCTION

Accessibility of hygienic and clean water is crucial to human health, sustainable economy and healthy environment. Environment pollution has always been a concern for society, especially water pollution. Pollution from heavy metals has grown to be a significant issue in the current scenario [1]. Most of the industries like pharmaceutical, fertilizers, metallurgy, smelting, aerospace, corrosion, photography, mining, electroplating, agricultural pesticides, surface finishing, iron, steel and fuel production discharge heavy metal ions either directly or indirectly into the water resources. Heavy metals like Cd(II), As(III), Ni(II), Zn(II), Pb(II), Cr(VI), Co(II), Hg(II), Cu(II) are highly toxic due to their persistence in the water [2]. WHO established the permissible concentration for heavy metal ions in water are 1.0-1.3 mg/L for Cd(II), 0.005-0.015 mg/L for Pb(II), 0.05-0.25 mg/L for Cr(III), 0.002 mg/L for Hg(II) and 5 mg/L for Zn(II) and beyond these limits, heavy metal ions are carcino-

genic and mutagenic. However, due to unregulated release of all of these contaminants in the water, values of concentration of Cd(II), Ni(II) and Pb(II) up to 0.01 mg/L, 0.20 mg/L and 0.006 mg/L were detected in different effluents [3]. These are directly affecting the ecosystem living even at extremely low concentration. Disposal of metal ions from wastewater are very necessary and proper treatment of these contaminants is major environmental concern.

The removal of toxic heavy metals from wastewater is of primary importance for health and environment. There are numbers of methods that are accessible for removal of heavy metals from polluted water. The conventional methods such as chemical precipitation, reverse osmosis, ion-exchange, nanofiltration, coagulation, ultrafiltration and flocculation have many limitations such as sensitive operating conditions, formation of sludge, which is costly to dispose and less effective at very low concentrations [4]. Compared to the previously described approaches, the use of biosorbent has increased in the

past several decades due to its high efficiency, simplicity, affordability and environmental friendliness [5].

Plant-based adsorbents of various types have recently been utilized to remove Pb(II), Cr(VI), Co(II), Ni(II) and Cd(II) from aqueous solutions. Several plants have been used as biosorbents in previous studies for remediation of heavy metals, including *Prosopis juliflora* [6], *Dicerocaryumerio carpum* [7], *Strychnos potatorum* L. [8], *Glebionis coronaria* L. and *Diplotaxis harra* [9], *Cassia fistula* [10] and *Pinus eldarica* [11]. The plant biomass is highly effective in eliminating metals ions due to its biochemical structure containing amino (-NH₂), acidic (-COOH) carboxyl (-C=O) and hydroxyl (-OH) functional groups, which participate during the adsorption process [12].

This study focussed on the biosorption of heavy metal ions such as Pb(II), Cd(II), Cr(VI) using *Aegle marmelos* leaves as a biosorbent from the synthetic wastewater. This plant has a great deal of attention in the science field because of its remarkable medical benefits and environmental uses. *A. marmelos* plant is native to the Indian subcontinent and this plant is now grown all over the world because it can thrive in arid, tropical and semi-tropical climates. Each of the parts of *A. marmelos* (Bael) such as its leaves, seeds, flowers and fruits are having vast groups of chemical compounds which are responsible for its distinctive characteristics. Polar groups including -NH₂, -COOH and -OH are present which are creating negative charge on *A. marmelos* biosorbent surface [13]. The surface structure of the leaf remains stable even after prolonged agitation treatment, which makes it an effective adsorbent. The present investigation is carried out to study the effectiveness of *A. marmelos* (Bael) leaves powder in biosorption of Cd(II), Cr(VI) and Pb(II) from the synthetic wastewater under batch studies using the adsorption isotherms.

EXPERIMENTAL

Biosorbents: *Aegle marmelos* leaves were collected from the Botanical garden, C.C.S. Haryana Agricultural University, Hisar, India. Leaves were first cleaned with tap water and then with double distilled water to eliminate dirt. After being cleaned, they were then under shade dried for 15 days then dried for 24 h at 100 °C in an oven. The dried leaves were ground into powdered form and sieved through 80 BSS stainless steel sieve. The powdered form was stored in a tightly sealed container for used in the later experiments as biosorbent.

Preparation of heavy metal ions solution: For the experiment, the stock solution of concentration 1000 mg/L of Pb²⁺, Cd²⁺ and Cr⁶⁺ metal ions were prepared by dissolving 1.598 g of Pb(NO₃)₂, 2.744 g of Cd(NO₃)₂·4H₂O and 2.7476 g of K₂Cr₂O₇ in 1 L of distilled water. All these chemicals were procured from Hi-media Laboratories Pvt. Ltd. The water samples for all experiments were prepared by diluting the stock solution to 20, 30, 40, 50, 60, 70 and 80 mg/L.

Characterization: The functionality of biosorbent was determined using Fourier Transform Infrared spectroscopy (Nicolet 50) in the range of 4000-400 cm⁻¹ through standard KBr method. For N₂ adsorption/desorption analysis of biosorbent, degassed for 24 h at 130 °C, (Quantachrome IQ-XR-XR, 2Stat.) using BET (Brunauer-Emmett-Teller) analysis. BET

equation was used to calculate surface area, the BJH model was employed to determine the total pore volume and the DFT model was used to determine the average pore size [14]. The surface morphology was studied by field emission scanning electron microscopy (JSM-761FPlus) technique using a Quanta 200F microscope with an accelerating voltage of 20 kV for analysis and biosorbent sample was coated with gold (Au) at argon pressure of 10⁻² mbar for 60 s in order to create a conductive layer on surface. Energy-dispersive X-ray spectroscopy (EDX) was used to observe the elements present in biosorbent before and after the adsorption [15].

Adsorption experiments: The batch experiments were conducted for biosorption of Cd(II), Cr(VI) and Pb(II) on biosorbent. In this study, the biosorption efficiency of biosorbent towards the heavy metal ions was examined by varying the different parameters, involving pH, initial concentration of metal ions, contact time and biosorbent dosage. To optimize pH, 20 mL solutions containing 20 ppm metal ions at different pH values (2, 3, 4, 5, 6, 7, 8 and 9) were prepared. Different amount of biosorbents, 0.01 g, 0.02 g, 0.04 g, 0.06 g, 0.08g, 0.1g and 0.2g were taken for optimization of biosorbent dose. To optimize the initial concentration, metal solutions were prepared at different concentrations (20, 30, 40, 50, 60, 70 and 80 ppm) and then allowed to interact for various time intervals of 30, 60, 90, 120, 150, 180 and 210 min, to optimize the initial concentration of metal ions and contact time. Then the mixtures were agitated in a rotary shaker set at 200 rpm at 30 °C. After each adsorption experiment was completed, the samples were separated into liquid and solid part by centrifugation at 4000-5000 rpm for 10-15 min. The flame atomic absorption spectroscopy (FAAS) technique (Thermo-Scientific) was used to calculate the concentrations C_e (mg/L) of Pb²⁺, Cr⁶⁺ and Cd²⁺ ions in solution. In FAAS, acetylene gas was used as fuel to produce flame. The maximum absorbance at a wavelength was set according to the metal ions were detected and 228.8 nm, 216.9 nm and 357.9 nm for Cd²⁺, Pb²⁺ and Cr⁶⁺ respectively. The quantity of metallic ions adsorbed per gram of adsorbent at equilibrium can be determined by eqn. 1:

$$q_e = \frac{(C_i - C_f)V}{m} \quad (1)$$

where, q_e is maximum adsorption capacity at equilibrium (mg/g) by biosorbent, C_f (mg/L) represents the metal ions concentration at equilibrium time t (min), C_i (mg/L) represents the initial metal ions concentration, V is the volume of the metal ions solution in litre and m is the mass of biosorbent (g).

The experimental data for Cd²⁺, Cr⁶⁺ and Pb²⁺ metal ions biosorption and heterogeneity or homogeneity of biosorbent was revealed by the Langmuir and Freundlich adsorption isotherm models. Linear and non-linear equations of Langmuir isotherm are represented by eqns. 2 and 3:

$$\frac{C_e}{q_e} = \frac{1}{K_L \times q_{\max}} + \frac{C_e}{q_{\max}} \quad (2)$$

$$q_e = \frac{K_L \times q_{\max} \times C_e}{1 + K_L \times C_e} \quad (3)$$

whereas the linear and nonlinear forms of Freundlich adsorption isotherm are represented in eqns. 4 and 5:

$$\log q_e = \log K_f + \frac{1}{n} \log C_e \quad (4)$$

$$q_e = K_f \times (C_e)^{1/n} \quad (5)$$

where C_e is the Langmuir constant (L/mg or M^{-1}), n is the heterogeneity factor; q_e is the adsorptive capacity at equilibrium; K_f is the Freundlich constant related to adsorption capacity (mg/g·(mg/L)ⁿ).

The descriptive adsorption process was also studied by using the pseudo-first-order and pseudo-second-order (linear and nonlinear) models. The following eqns. 6 and 7, describe these models, respectively:

$$q_t = q_e(1 - e^{-K_1 t}) \quad (6)$$

$$q_t = \frac{(q_e^2 K_2 t)}{(q_e K_2 t + 1)} \quad (7)$$

where K_1 and K_2 are the pseudo-first-order and pseudo-second-order constant [16].

RESULTS AND DISCUSSION

FTIR studies: The FTIR spectra of *A. marmelos* biosorbent before and after metal biosorption show the negligible difference in peak intensity and position as shown in Fig. 1. The broad peak at 3450-3300 cm^{-1} corresponds to the -OH stretching and is probably related to the presence of cellulosic groups, lignin and carbohydrates present in biosorbent. The peak appearing at 2950-2800 cm^{-1} is probably due to the presence of asymmetric and symmetric stretching of C-H bonds, which indicates the presence of lipid content [17]. The C=O stretching peak is present at 1650-1600 cm^{-1} , whereas the peaks at 1450-1400 cm^{-1} and 1250 cm^{-1} can be attributed to the highly asymmetric -COO and -CH₃ groups (due to proteins). Furthermore, the peaks at 890.3 cm^{-1} , 1050-1000 cm^{-1} and 766.63 cm^{-1} can be attributed to the asymmetric stretching of C-C, the C=O bond of the carboxylic acid group and the strong bending vibration

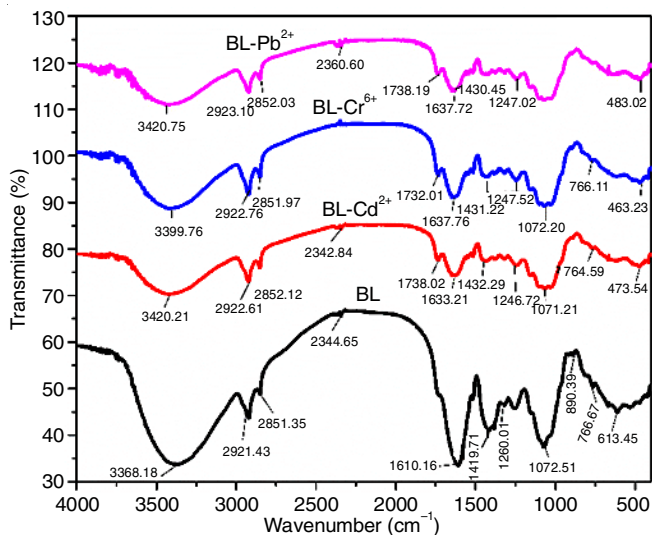


Fig. 1. FTIR spectra of raw biosorbent and Cd²⁺, Cr⁶⁺, Pb²⁺ loaded biosorbent

of the alkyne [18]. After biosorption, peak was observed at 500-450 cm^{-1} due to metal ions present in biosorbent. It was observed that there was no substantial change in the band shift after adsorption of metal ions, suggesting that the possibility of complex formation with metal ions unlikely to take place. As a result, the ion exchange between the functional groups on the surface of the biosorbents and the metal ions may take place [4].

FESEM and EDX: The SEM images of biosorbent after and before sorption are shown in Fig. 2. Before sorption, the biosorbent had non-uniform and porous surface, which was shown to have a large number of voids on the biosorbent surface. After adsorption, heterogeneity of the surface reduced and the adsorption of some ions were revealed on the biosorbent surface [19].

BET analysis: BET equation was used to find out surface area, the BJH model was employed to determine the total pore volume and pore size and DFT model was used to determine the average pore size. N₂ adsorption-desorption isotherm and distribution of pore sizes for biosorbent presented in Fig. 3. BET surface area (m²/g), pore volume and pore diameter of biosorbent were found to be 6.97 m² g⁻¹, 0.004 cm³ g⁻¹ and 0.004 Å, respectively, similar results were observed in previous research work [20]. Based on the IUPAC classification, the N₂ adsorption/desorption isotherm of biosorbent exhibits a type IV isotherm and H3 hysteresis [21].

Batch studies

Effect of pH: The initial pH value of metal ion solution has a significant influence on the biosorption of metal ions on the binding sites of biosorbent surface. The biosorption removal efficiency of Cd(II), Cr(VI) and Pb(II) at 20 mg/L initial metal ion concentration, using 0.02 g/20 mL solution and varying the pH in the range 2 to 9. The contact time was kept constant at 60 min. It was revealed that the removal of chromium metal ions was most effective at a pH of 3. This is because, at low pH, the functional groups on the biosorbent surface became protonated. The metal ions Cr(VI) carries a high negative charge density due to the presence of oxy ions Cr₂O₇²⁻ and CrO₄²⁻ in solution, resulting in a strong electrostatic interaction between the positively charged surface of the biosorbents and the oxy-anions or Cr(VI). However, as the pH increased, this interaction decreased due to the presence of negative charges on the biosorbent surface and the increased presence of highly negatively charged OH⁻ ions. At high pH levels, there was competition between oxy ions and hydroxide ions for the adsorption sites, resulting in decreased removal efficiency after pH 3. The efficiency of removing Pb(II) and Cd(II) metal ions was found to increase up to pH 6 and then decline. This is because at low pH levels, there are excess H⁺ ions in the solution, leading to greater competition between metal ions and H⁺ ions for active sites. As the pH of solution increases, the surface of biosorbent becomes negatively charged, resulting in increased attraction of metal ions and H⁺ ions. However, beyond the optimum condition, further increase in the pH of solution led to decreased removal efficiency due to the formation of precipitation of Pb(II) and Cd(II) as Pb(OH)₂ and Cd(OH)₂ in the solution.

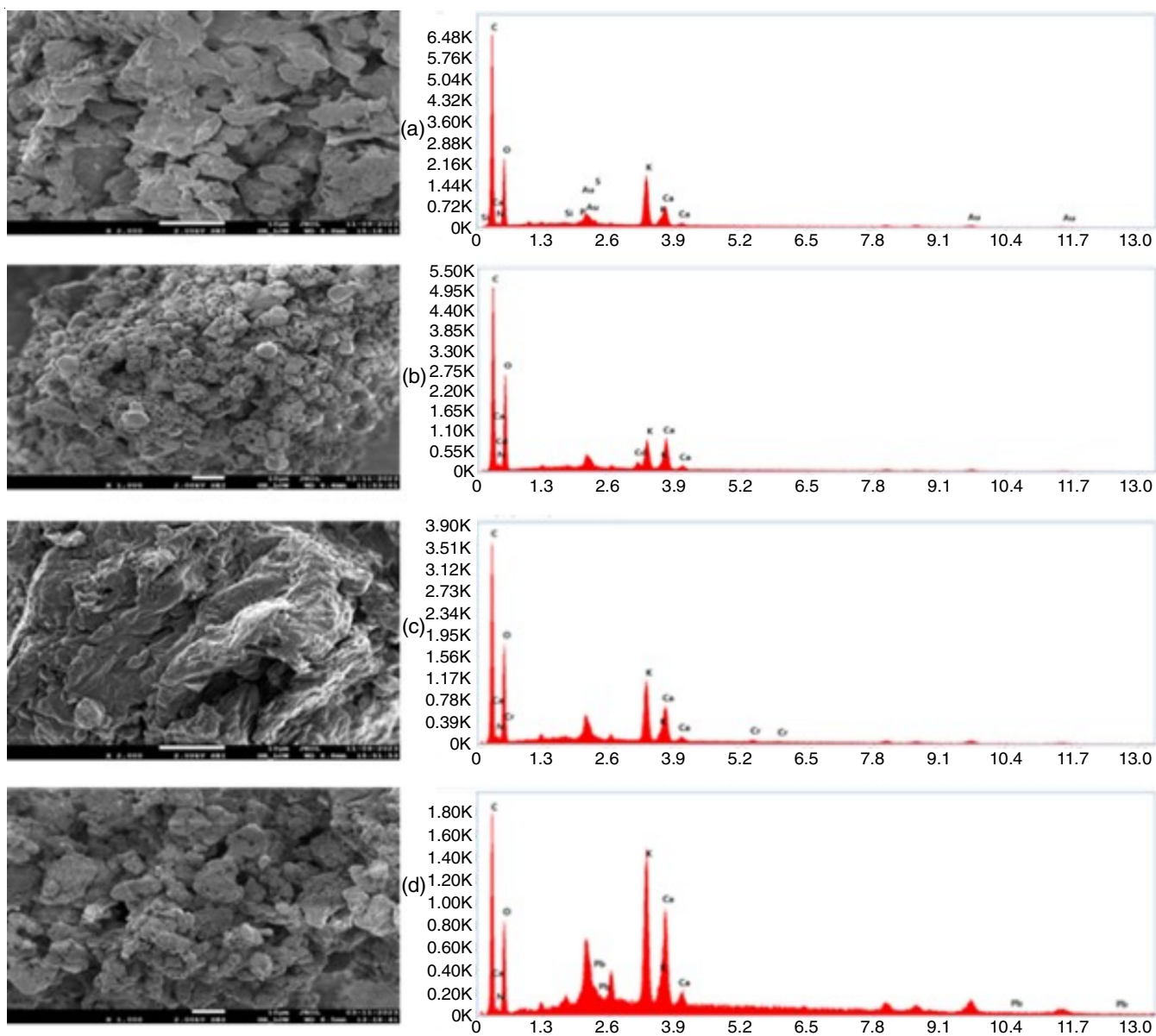


Fig. 2. FE-SEM micrograph of biosorbent (a) Raw, (b) Cd, (c) Cr and (d) Pb loaded biosorbent

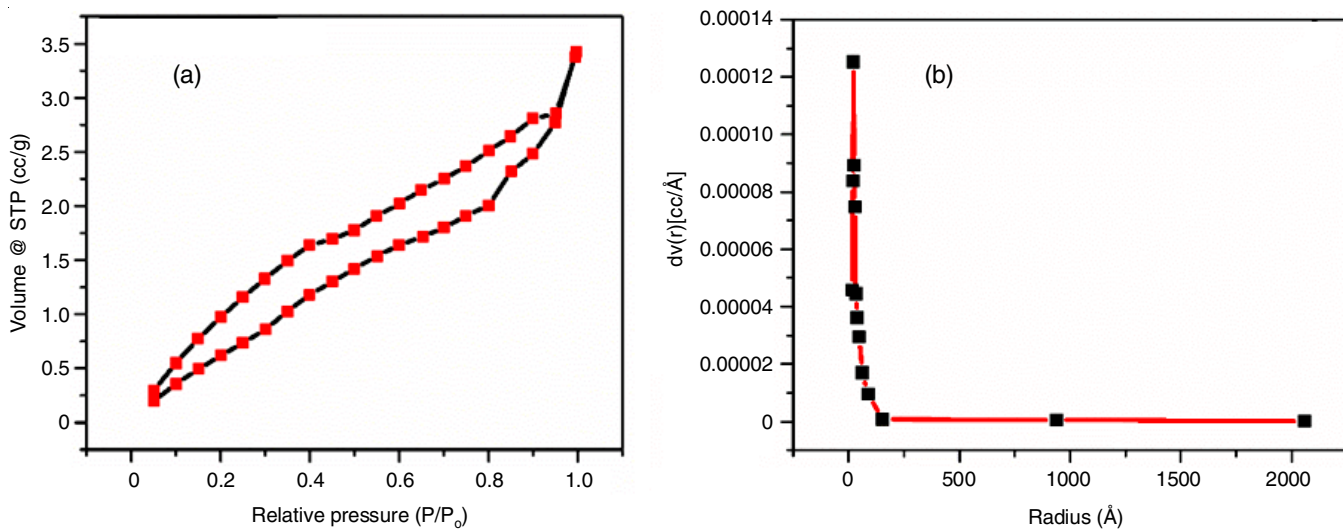


Fig. 3. (a) N_2 adsorption-desorption isotherm and (b) distribution of pore sizes for biosorbent

The removal efficiency for Cr(VI) at pH 3 was 39% and for Pb(II) and Cd(II) were 44% and 33%, respectively as shown in Fig. 4. The optimal pH value for biosorption of Cr(VI) at 3 and 6 for Cd(II) and Pb(II) was observed. Similar results were also observed for Cr(VI), Cd(II), Zn(II), Cu(II) and Pb(II) from aqueous solutions using *Allium cepa* seeds as biosorbent [22].

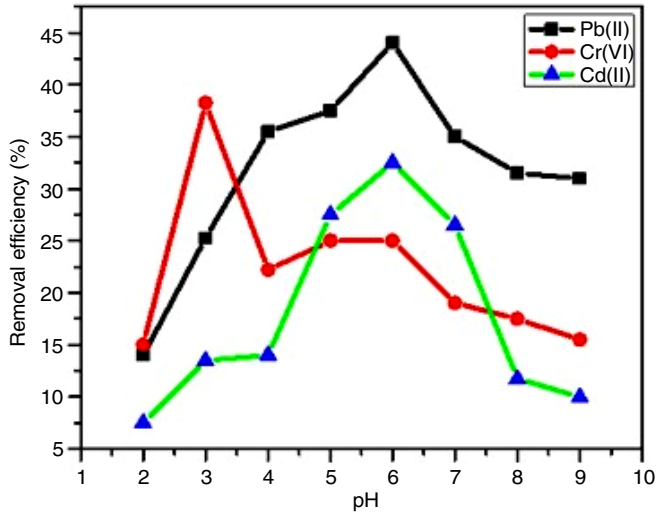


Fig. 4. Graph between pH vs. removal efficiency (%)

Effect of dose: The removal efficiency of heavy metal ions from wastewater also depend on the biosorbent dose. The effect of the biosorbent dose was studied at 0.02-0.2 g at optimum pH 6 for Pb(II) and Cd(II) and at optimum pH 3 for Cr(VI), with initial metal ion concentration 20 mg/L and contact time 60 min. A prominent increase in biosorption efficiency of metal ions with increase in the biosorbent dose due to the availability of more surface area and active sites for the biosorption of heavy metal ions. As shown in Fig. 5, the efficiency of removing Cr(VI), Cd(II) and Pb(II) ions increases up to a dosage of 0.06 g. Beyond this dosage, there was no significant change in the sorption efficiency due to the aggregation of biosorbent particles and a decrease in active sites on the biosorbent surface. It was observed that Pb(II) showed the high adsorption capacity com-

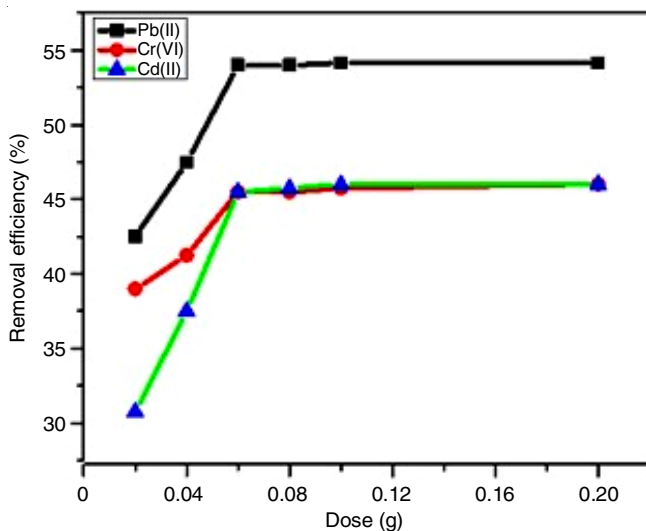


Fig. 5. Graph between biosorbent dose vs. removal efficiency (%)

pared to the Cd(II) and Cr(VI) when utilizing an equal amount of adsorbent because Pb(II) metal ion have higher ionic radius than Cd(II) and Cr(VI) and the smaller hydrated radius as compared to the Cd(II) and Cr(VI) metal ions in the aqueous solution. So, the removal efficiency and adsorption capacity exhibited by biosorbent for Pb(II) over Cd(II).

Effect of metal ions concentration: The impact of varying initial metal ion concentrations (20-80 mg/L) on the efficiency of biosorption of biosorbent at optimized biosorbent dosage and pH. It was observed that the biosorption efficiency for Cr(VI), Pb(II) and Cd(II) increases up to 52%, 70% and 62.5% respectively, as the initial concentration of the metal ions rises and beyond the metal concentration 40 mg/L, the biosorption efficiency tends to decrease (Fig. 6). These patterns are possibly from the concept that large proportion of active sites to the all metal ions present in solution, an increased probability of interaction between metal ions and the biosorbent leads to greater biosorption. This leads to maximum adsorption on the surface of biosorbent. However, at higher metal ion concentration, the binding sites of the biosorbent will rapidly reach saturation due to the constant amount of biosorbent available. The pH of solution get decrease, when active sites of the biosorbents saturated by ions of heavy metal. This suggest that during the binding process, the H^+ releases into the solution and the pH of solution gets decrease, removal efficiency of the metal ions decrease.

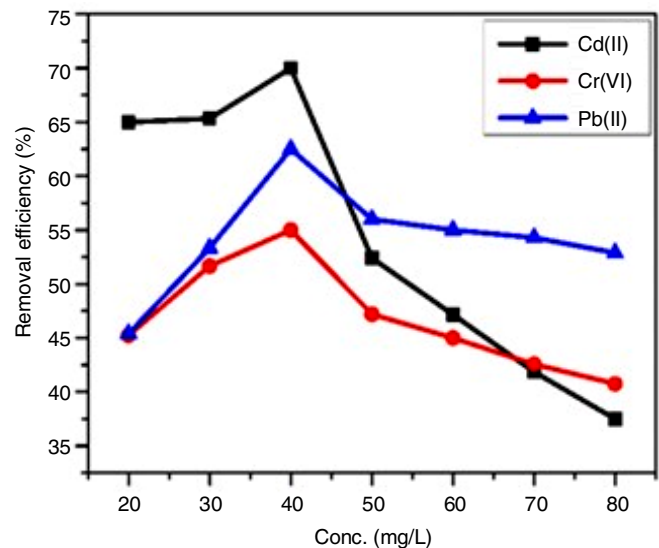


Fig. 6. Graph between concentration vs. removal efficiency (%)

Effect of contact time: The removal efficiency of Cd^{2+} , Cr^{6+} and Pb^{2+} metal ions at different contact time (30, 60, 90, 120, 150, 180, 210 min) at 30 °C was studied. It was observed that there is a gradual increase in the removal efficiency as time was increased up to 120 min and then attained equilibrium. On further increasing the contact time, there was no discernible change in the percentage removal efficiency as shown in Fig. 7. Initially, there are availability of unoccupied sites on biosorbent surface. After that equilibrium was reached, due to the biosorbent surface's open sites gradually being exhausted [23]. Removal efficiency of biosorbent for Pb^{2+} , Cr^{6+} and Cd^{2+} ions were found 75.8%, 58.8% and 70%, respectively.

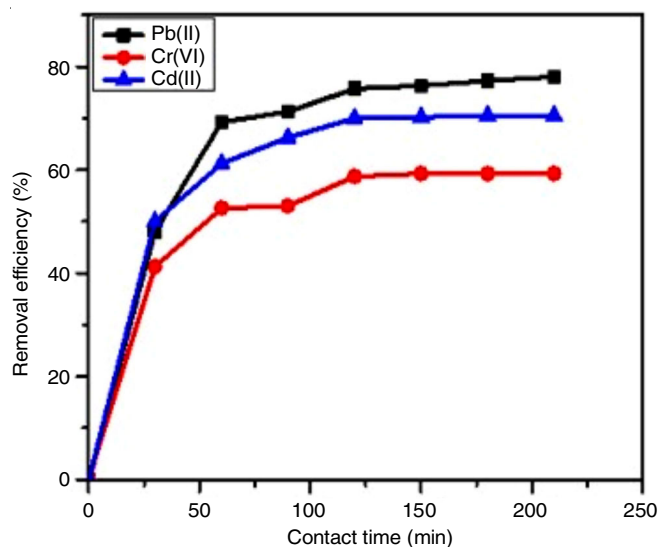


Fig. 7. Graph between contact time vs. removal efficiency (%)

Adsorption studies: Based on the equilibrium data, Freundlich's and Langmuir models were utilized to determine whether the heavy metal ions adsorbed in the monolayer or multilayer form on the biosorbent surface. Isotherm refers to the relationship between equilibrium metal ions concentration in solution and equilibrium amount of metal ions on the adsorbent at certain temperature. The regression coefficients (R^2) was used to select the best adsorption isotherm. The data fit well with the Langmuir model, with regression coefficients (R^2) of 0.93, 0.92 and 0.95 for Cd(II), Cr(VI) and Pb(II), respectively and the maximum monolayer adsorption capacities (q_{max}) for Cd(II), Cr(VI) and Pb(II) were found to be 21.5, 18.2 and 29.75 mg/g, respectively (Table-1), which were higher than the Freundlich adsorption isotherm. These results were confirmed that biosorption follow the Langmuir isotherm and has monolayer adsorption on the homogenous surface of biosorbents, which have finite numbers of active sites [24].

Kinetics studies: The effect of contact time of Pb(II), Cr(VI) and Cd(II) onto was investigated at different temperature *i.e.* 303 K, 313 K and 323 K.

TABLE-1
LINEAR AND NON-LINEAR PARAMETERS FOR
FREUNDLICH AND LANGMUIR ISOTHERM

Isotherm models	Parameter	Cd(II)	Cr(VI)	Pb(II)
Freundlich (non-linear)	N	1.58	1.66	1.11
	K_F (mg/g)(L/mg) ^{1/n}	0.97	1.04	0.56
	R^2	0.85	0.91	0.89
Freundlich (linear)	N	1.72	1.56	0.92
	K_F (mg/g)(L/mg) ^{1/n}	0.025	0.083	0.030
	R^2	0.85	0.83	0.84
Langmuir (non-linear)	q_m (mg/g)	21.5	18.2	29.75
	K_L (L/mg)	0.023	0.026	0.05
	R^2	0.93	0.93	0.95
Langmuir (linear)	q_m (mg/g)	18.5	17.2	32.55
	K_L (L/mg)	0.022	0.026	0.041
	R^2	0.87	0.84	0.80

In order to understand the kinetic behaviour of metal ion adsorption onto biosorbents, the pseudo first-order (PFO) and pseudo-second-order (PSO) models were attempted. As the temperature increased from 303 K to 323 K, the removal efficiency and adsorption capacity also increased, which suggests that the adsorption process is endothermic. Similarly, others have also reported the endothermic nature of the adsorbent. The experimental data indicates that as the temperature increased, the number of active sites on the biosorbent also increased, while the bounding layer surrounding the biosorbent decreased. From the experimental data, the regression coefficient value in pseudo-second order were close to unity in all cases and maximum uptake of metal ions by adsorbent. It was observed that experimental equilibrium data best fitted into the pseudo-second-order kinetics for all three metal ions Pb(II), Cr(VI) and Cd(II) and demonstrated evidence of chemisorption [25]. The regression coefficient (R^2) and rate constant in linear and nonlinear pseudo first and second orders for Cd(II), Cr(VI) and Pb(II) are shown in Table-2.

Based on the values of maximum adsorption capacity obtained, the Langmuir model proposed the following order: Pb(II) > Cd(II) > Cr(VI). Removal efficiency of biosorbent for Pb²⁺, Cr⁶⁺ and Cd²⁺ ions were found 76%, 58.8% and 70%,

TABLE-2
LINEAR AND NON-LINEAR PARAMETERS KINETIC MODELS FOR THE BIOSORPTION OF
Pb(II), Cd(II) AND Cr(VI) METAL IONS ON DIFFERENT TEMPERATURE

Kinetics models	Parameter	Pb(II)			Cd(II)			Cr(VI)		
		303 K	313 K	323 K	303 K	313 K	323 K	303 K	313 K	323 K
PFO (non-linear)	$q_{e,cal}$ (mg/g)	8.695	9.866	11.121	8.81	8.95	9.11	6.71	7.31	7.40
	K_1 (min ⁻¹)	0.0277	0.0305	0.0326	0.017	0.018	0.019	0.052	0.05	0.05
	R^2	0.98	0.94	0.98	0.98	0.98	0.98	0.92	0.85	0.86
PFO (linear)	$q_{e,cal}$ (mg/g)	6.062	7.731	5.316	1.937	2.564	2.409	1.94	2.56	2.41
	K_1 (min ⁻¹)	0.0175	0.0241	0.0155	0.0135	0.0087	0.0094	0.014	0.008	0.009
	R^2	0.98	0.95	0.93	0.9390	0.9245	0.9449	0.94	0.93	0.95
PSO (non-linear)	$q_{e,cal}$ (mg/g)	10.133	11.277	12.656	11.0	11.25	11.56	7.19	8.00	8.16
	K_2 (g/mg min ⁻¹)	0.0035	0.00374	0.00365	0.0016	0.0015	0.0013	0.01434	0.0097	0.01
	R^2	0.9877	0.9545	0.9856	0.97	0.98	0.99	0.98	0.98	0.99
PSO (linear)	$q_{e,cal}$ (mg/g)	10.046	11.087	12.387	7.181	8.000	8.056	7.1	8.01	8.1
	K_2 (g/mg min ⁻¹)	0.0036	0.0041	0.0041	0.0145	0.0094	0.0102	0.0146	0.0095	0.01
	R^2	0.9995	0.9978	0.9967	0.9996	0.9997	0.9999	0.99	0.99	0.99

PFO = pseudo first-order; PSO = pseudo-second-order

respectively at equilibrium time 120 min. Adsorption model isotherm Langmuir non-linear isotherm was best fitted with R^2 value 0.93, 0.92 and 0.95 for Cd^{2+} , Cr^{6+} and Pb^{2+} ions, respectively. The result is consistent with the finding reported for the removal of metal ions from water using different biomass adsorbents [25].

Thermodynamic studies: Temperature significantly impacts the adsorption of metal ions on bael leaves biosorbent. The free energy change (ΔG°), entropy change (ΔS°) and enthalpy change (ΔH°) were calculated to investigate the effect of temperature on the adsorption of heavy metal ions on the modified biosorbent. The equilibrium constant (K_c) calculated by following eqn. 8:

$$K_c = \frac{q_e}{C_e} \quad (8)$$

where q_e = adsorption capacity (mg/g) at equilibrium and C_e = concentration (mg/L) at equilibrium.

The thermodynamics parameters were calculated by using following van't Hoff's equation (eqn. 9):

$$\ln K_c = \frac{\Delta S^\circ}{R} - \frac{\Delta H^\circ}{RT} \quad (9)$$

and

$$\Delta G^\circ = \Delta H^\circ - T\Delta S^\circ \quad (10)$$

where ΔG° = Gibb's free energy change, T = temperature, ΔH° = change in enthalpy and ΔS° = change in entropy in adsorption process.

In Table-3, specifically, the value of ΔG° increased as the temperature increased from 303 K to 323 K for the adsorption of Cd^{2+} , Cr^{6+} and Pb^{2+} ions, which showed that adsorption process was more favourable at high temperature and the negative values of ΔG° for the adsorption of all the metal ions indicate that the adsorption process was feasible and spontaneous. The positive values of ΔH° and ΔS° were reported for the all the metal ions for the bael leaves. The adsorption process was found to be spontaneous, feasible and endothermic. The positive value of the entropy was showed that better affinity of the metal ions on the surface of adsorbent [26].

The biosorbent showed higher removal efficiency for Pb^{2+} than Cd^{2+} and Cr^{6+} . This is due to the fact that Pb^{2+} has a smaller hydrated radius (0.401 nm) than Cr^{6+} , which has a higher hydra-

tion radius. Smaller metal ions have higher hydration energy, hence, the removal efficiency of Cr^{6+} is less than Pb^{2+} and Cd^{2+} [12].

Conclusion

In this study, the removal efficiency of Cd^{2+} , Cr^{6+} , Pb^{2+} heavy metals ions was examined by using *Aegle marmelos* leaves as biosorbent. The biosorption capacity of all the metal ions depends on various factors such as pH, metal concentration, contact time and biosorbent dose. Removal efficiency of biosorbent for Pb(II), Cd(II) and Cr(VI), metal ions were found 76%, 70% and 58.8%, respectively at equilibrium time 120 min. Langmuir isotherm was best fitted with R^2 value 0.93, 0.92 and 0.95 and the maximum adsorption capacity was 29.75 mg/g, 21.5 mg/g and 18.2 mg/g for Pb(II), Cd(II) and Cr(VI) heavy metal ions, respectively. According to the kinetics models, adsorption follow better linear pseudo-second order, which showed that the adsorption process is the chemisorption. The thermodynamics studies evaluated the adsorption process was spontaneous and endothermic. Finally, removal efficiency of *Aegle marmelos* leaves biosorbent against the all three studied metals were found maximum for Pb^{2+} followed by Cd^{2+} and Cr^{6+} due to variation in hydration energy of three heavy metals. It was concluded that low cost *A. marmelos* leaves could be used as biosorption for pollutants removal from the wastewater.

CONFLICT OF INTEREST

The authors declare that there is no conflict of interests regarding the publication of this article.

REFERENCES

- W.S. Chai, J.Y. Cheun, P.S. Kumar, M. Mubashir, Z. Majeed, F. Banat, S.H. Ho and P.L. Show, *J. Clean. Prod.*, **296**, 126589 (2021); <https://doi.org/10.1016/j.jclepro.2021.126589>
- E. Burakov, E.V. Galunin, I.V. Burakova, A.E. Kucherova, S. Agarwal, A.G. Tkachev and V.K. Gupta, *Ecotoxicol. Environ. Saf.*, **148**, 702 (2018); <https://doi.org/10.1016/j.ecoenv.2017.11.034>
- M. Shafiq, A.A. Alazba and M.T. Amin, *Sains Malays.*, **47**, 35 (2018); <https://doi.org/10.17576/jsm-2018-4701-05>
- M.M. Ali and J.N. Bhakta, *Water Environ. Res.*, **92**, 821 (2020); <https://doi.org/10.1002/wer.1274>
- B.D. Pant, D. Neupane, D.R. Paudel, P. Chandra Lohani, S.K. Gautam, M.R. Pokhrel and B.R. Poudel, *Heliyon*, **8**, e09283 (2022); <https://doi.org/10.1016/j.heliyon.2022.e09283>

TABLE-3
THERMODYNAMICS PARAMETERS STUDIES FOR THE Cr(VI), Cd(II) AND Pb(II)

Temp. (K)	1/T	K_c	$\ln K_c$	ΔG° (KJ/mol)	R^2	ΔH° (KJ/mol)	ΔS° (J/K/mol)
Cd(II)							
303	0.0033003	1.75	0.5596	-1.41	0.81	14.43	52.55
313	0.0031948	2.32	0.8416	-2.19			
323	0.0030956	2.49	0.9122	-2.45			
Cr(VI)							
303	0.0033003	1.63	0.4886	-1.23	0.79	14.98	53.79
313	0.0031948	2.20	0.7885	-2.05			
323	0.0030956	2.35	0.8544	-2.29			
Pb(II)							
303	0.0033003	2.25	0.8109	-2.04	0.99	10.60	41.74
313	0.0031948	2.58	0.9478	-2.47			
323	0.0030956	2.92	1.0715	-2.88			

6. K. Gautam, N.B. Markandeya, N.B. Singh, S.P. Shukla and D. Mohan, *SN Appl. Sci.*, **2**, 288 (2020); <https://doi.org/10.1007/s42452-020-2065-0>
7. B.O. Jones, O.O. John, C. Luke, A. Ochieng and B.J. Bassey, *Environ. Manag. Today*, **177**, 365 (2016); <https://doi.org/10.1016/j.jenvman.2016.04.011>
8. K. Jayaram, I.Y.L.N. Murthy, H. Lalhruiatluanga and M.N.V. Prasad, *Colloids Surf. B Biointerfaces*, **71**, 248 (2009); <https://doi.org/10.1016/j.colsurfb.2009.02.016>
9. H. Tounsadi, A. Khalidi, M. Abdennouri and N. Barka, *J. Environ. Chem. Eng.*, **3**, 822 (2015); <https://doi.org/10.1016/j.jece.2015.03.022>
10. R.R.V. Hemavathy, P.S. Kumar, S. Suganya, V. Swetha and S.J. Varjani, *Bioresour. Technol.*, **281**, 1 (2019); <https://doi.org/10.1016/j.biortech.2019.02.070>
11. S. Asgarzadeh, R. Rostamian, E. Faez, A. Maleki and H. Daraei, *Desalination Water Treat.*, **57**, 14544 (2016); <https://doi.org/10.1080/19443994.2015.1067831>
12. M. Abatal, M.T. Olguin, I. Anastopoulos, D.A. Giannakoudakis, E.C. Lima, J. Vargas and C. Aguilar, *Coatings*, **11**, 508 (2021); <https://doi.org/10.3390/coatings11050508>
13. S. Baruah, A. Devi, K.G. Bhattacharyya and A. Sarma, *Int. J. Environ. Sci. Technol.*, **14**, 341 (2017); <https://doi.org/10.1007/s13762-016-1150-9>
14. P. Sinha, A. Datar, C. Jeong, X. Deng, Y.G. Chung and L.C. Lin, *J. Phys. Chem. C*, **123**, 20195 (2019); <https://doi.org/10.1021/acs.jpcc.9b02116>
15. M.A. Mutalib, M.A. Rahman, M.H.D. Othman, A.F. Ismail and J. Jaafar, in eds.: N. Hilal, A.F. Ismail, T.i Matsuura and D. Oatley-Radcliffe, *Scanning Electron Microscopy (SEM) and Energy-Dispersive X-Ray (EDX) Spectroscopy*, In: *Membrane Characterization*, Elsevier, Chap. 9, pp. 161-179 (2017).
16. M.A. Al-Ghouti and D.A. Da'ana, *J. Hazard. Mater.*, **393**, 122383 (2020); <https://doi.org/10.1016/j.jhazmat.2020.122383>
17. G. Yashni, A. Al-Gheethi, R.M.S.R. Mohamed, V. Abirama Shanmugan and J. Abu Bakar, *Mater. Today Proc.*, **47**, 1345 (2021); <https://doi.org/10.1016/j.matpr.2021.02.829>
18. G. Yuvaraja, N. Krishnaiah, M.V. Subbaiah and A. Krishnaiah, *Colloids Surf. B Biointerfaces*, **114**, 75 (2014); <https://doi.org/10.1016/j.colsurfb.2013.09.039>
19. J.O. Ighalo and A.G. Adeniyi, *SN Appl. Sci.*, **2**, 509 (2020); <https://doi.org/10.1007/s42452-020-2335-x>
20. R. Hassan, H. Arida, M. Montasser and N.A. Latif, *J. Chem.*, **2013**, 240568 (2013); <https://doi.org/10.1155/2013/240568>
21. D. Kolodyńska, J.A. Krukowska and P. Thomas, *Chem. Eng. J.*, **307**, 353 (2017); <https://doi.org/10.1016/j.cej.2016.08.088>
22. Z. Sheikh, M. Amin, N. Khan, M.N. Khan, S.K. Sami, S.B. Khan, I. Hafeez, S.A. Khan, E.M. Bakhsh and C.K. Cheng, *Chemosphere*, **279**, 130545 (2021); <https://doi.org/10.1016/j.chemosphere.2021.130545>
23. A.M. Kenawy, M.A.H. Hafez, M.A. Ismail and M.A. Hashem, *Int. J. Biol. Macromol.*, **107**, 1538 (2018); <https://doi.org/10.1016/j.ijbiomac.2017.10.017>
24. G. El-Chaghaby, S. Rashad and S. Abd-El-Kader, *Egypt. J. Bot.*, **60**, 707 (2020); <https://doi.org/10.21608/ejbo.2020.26449.1476>
25. M.J. Zamzow, B.R. Eichbaum, K.R. Sandgren and D.E. Shanks, *Sep. Sci. Technol.*, **25**, 1555 (1990); <https://doi.org/10.1080/01496399008050409>
26. Z. Harrache, M. Abbas, T. Aksil and M.Trari, *Microchem. J.*, **144**, 180 (2019); <https://doi.org/10.1080/01496399008050409>